Acta Cryst A
FOUNDATIONS
ADVANCES

ISSN 2053-2733

Received 2 November 2021
Accepted 6 December 2021

Edited by A. Altomare, Institute of Crystallography - CNR, Bari, Italy

Keywords: minimal surfaces; hyperbolic geometry; symmetry groups; subgroup lattices; conventional unit cells.

Supporting information: this article has supporting information at journals.iucr.org/a

The intrinsic group–subgroup structures of the Diamond and Gyroid minimal surfaces in their conventional unit cells

Martin Cramer Pedersen,[a]* Vanessa Robins[b] and Stephen T. Hyde[c]

[a]Niels Bohr Institute, University of Copenhagen, Denmark, [b]Research School of Physics, Australian National University, Australia, and [c]School of Chemistry, University of Sydney, Australia. *Correspondence e-mail: mcpe@nbi.ku.dk

The intrinsic, hyperbolic crystallography of the Diamond and Gyroid minimal surfaces in their conventional unit cells is introduced and analysed. Tables are constructed of symmetry subgroups commensurate with the translational symmetries of the surfaces as well as group–subgroup lattice graphs.

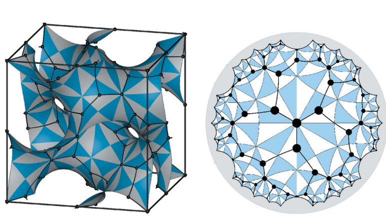

1. Introduction

The Primitive, Diamond (Schwarz, 1890) and Gyroid (Schoen, 1970) minimal surfaces are well known structures in the context of materials science, where they emerge in simulations of and experiments on a variety of systems ranging from butterfly wing scales (Dolan *et al.*, 2015) and biological detergent systems (Mezzenga *et al.*, 2019) to bulk polymer phases (Castelletto & Hamley, 2004).

Their crystallographic properties are well documented (Sadoc & Charvolin, 1989; Robins *et al.*, 2004; Hyde *et al.*, 2014) though only for the primitive unit cell of the side-preserving translation group. However, many applications such as molecular simulations (Kirkensgaard *et al.*, 2014), field theory based approaches (Welch *et al.*, 2019) or meshing algorithms (Pellé & Teillaud, 2014) rely on mutually orthogonal lattice vectors of equal length, corresponding to the conventional unit cells of these surfaces. The results from such computations are therefore better analysed in the conventional unit-cell settings (Fig. 1).

Here, we extend previous results on the intrinsic (hyperbolic) crystallography of these surfaces (Robins *et al.*, 2004) to these settings; we introduce canonical versions of their conventional unit cell in the universal covering space, $\mathbb{H}^2$, along with the group theory needed to construct the related translational subgroups. We derive the group–subgroup structure of the symmetries commensurate with the surfaces in these settings. We label our groups by their orbifold symbols which are explained at length in the literature (Thurston, 1980; Conway *et al.*, 2008; Hyde *et al.*, 2014).

For completeness, we include the Primitive surface in our calculations and tables but stress that these are identical to the ones presented earlier (Robins *et al.*, 2004), as the primitive and conventional unit cells of the Primitive surface coincide. We note that recent changes to *GAP*'s enumeration algorithms mean that our ordering differs slightly from the previous report.

2. Preliminaries and method

The intrinsic symmetry group of these three minimal surfaces can be labelled with the orbifold symbol $*246$. Similarly, upon compactification by pairwise identifying sides of the unit cells in Fig. 1, the resulting surfaces are the (genus-3) tritorus, the (genus-9) enneatorus and the (genus-5) pentatorus, respectively. Hence, the Conway orbifold symbols $\circ^3$, $\circ^9$ and $\circ^5$ describe the related translational groups.

We list the translations needed to construct the translational subgroups corresponding to the domains in Fig. 1 in the supporting information along with additional information and data on these groups.

Next, we construct and analyse all symmetry groups of the surfaces by the procedure described by Robins *et al.* (2004) using the methods outlined below along with the data presented in the supporting information. First, all subgroups

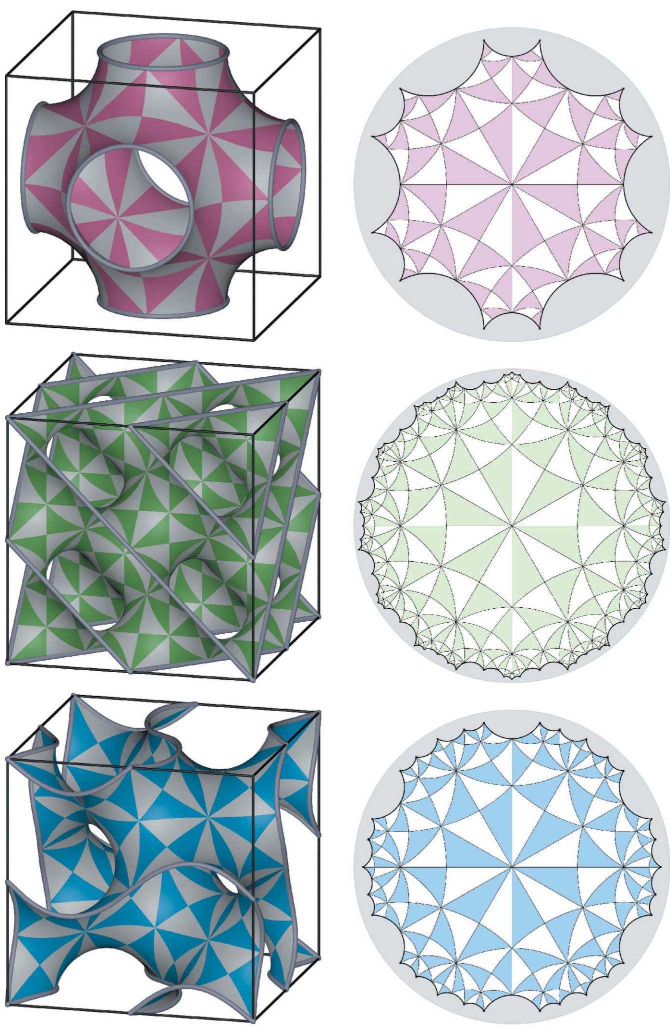

Figure 1
Left: the Primitive (top), Diamond (middle) and Gyroid (bottom) minimal surfaces oriented in their conventional unit cells with space groups $Pm\bar{3}m$, $Fd\bar{3}m$ and $I4_132$, respectively. Right: corresponding translational patches in the universal covering space, $\mathbb{H}^2$, visualized using the Poincaré disc model of $\mathbb{H}^2$. The combinatorics and group theory of the compactification of these patches as well as their coordinates can be found in the supporting information.

Table 1
The number of subgroups per index in $*246/\mathrm{T}$, where T is the translational subgroup for the given surface in its conventional unit cell.

The entries assigned a dash, –, are not combinatorially possible for the respective surface/group.

		Primitive	Diamond	Gyroid
Subgroup index	Euler characteristic	$*246/\circ^3$	$*246/\circ^9$	$*246/\circ^5$
1	$-\frac{1}{24}$	1	1	1
2	$-\frac{1}{12}$	7	7	7
3	$-\frac{1}{8}$	1	1	1
4	$-\frac{1}{6}$	8	8	12
6	$-\frac{1}{4}$	15	15	15
8	$-\frac{1}{3}$	8	10	14
12	$-\frac{1}{2}$	39	55	47
16	$-\frac{2}{3}$	7	14	12
24	-1	32	128	64
32	$-\frac{4}{3}$	1	10	7
48	-2	11	135	41
64	$-\frac{8}{3}$	–	7	1
96	-4	1	57	11
128	$-\frac{16}{3}$	–	1	–
192	-8	–	13	1
384	-16	–	1	–
Total		131	463	234

for a given surface (represented via the quotient group labelled $*246/\mathrm{T}$, where T is the appropriate translational subgroup) are computed using *GAP* and *KBMag* (Epstein *et al.*, 1991; The GAP Group, 2021). Then, for each subgroup, its generators are identified and the associated cosets are calculated. From these cosets, the Delaney–Dress (Dress, 1987; Delgado-Friedrichs, 2003) and orbifold symbols of the subgroup are computed. The suite of resulting groups describe all possible intrinsic symmetry groups of the parent minimal surfaces whose translations are those of their conventional unit cells.

3. Results and discussion

The results of our enumeration can be found in Table 1. Expanded tables containing detailed information on each subgroup can be found in the supporting information alongside group–subgroup lattice graphs outlining the structure of our three quotient groups.

We note that the translational domains shown in Fig. 1 and the corresponding translations listed in the supporting information are not unique. One can represent the pentatorus as *e.g.* a 20-gon rather than the outlined 30-gon, and accordingly the enneatorus can be represented as a 36-gon rather than our 60-gon. However, we retain the sixfold symmetry around the origin for easier subsequent analysis.

Changing translational symmetries of the primitive unit cells to those of the conventional unit cells admits additional symmetry groups on the surfaces. Fig. 2 shows an example of a trivalent net on the Gyroid which respects the translations of the conventional, but not the primitive, unit cell of that surface. The specific decoration and its embeddings in $\mathbb{H}^2$ and

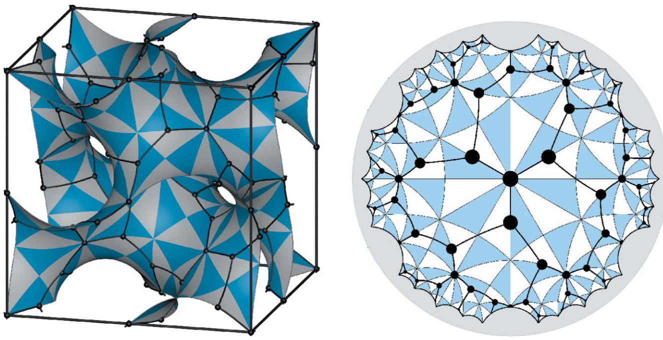

Figure 2
Left: an [8, 3] Schwarzite net on the Gyroid with intrinsic symmetry 23∗, subgroup No. 222 in the table for the Gyroid in the supporting information. The net – or rather its symmetry – is not commensurate with the primitive unit cell yet can be embedded in $\mathbb{E}^3$ via the conventional unit cell. Right: the same net shown in the universal covering space, $\mathbb{H}^2$. Crystallographic information on the canonical embedding (Delgado-Friedrichs & O'Keeffe, 2003) of this net can be found in the supporting information.

on the Gyroid were derived as outlined elsewhere (Pedersen & Hyde, 2018; Hyde & Pedersen, 2021). Whereas the primitive cells admit 131 distinct groups, the enlarged unit cells of the Diamond and Gyroid surfaces include 463 and 234 groups, respectively, each associated with a three-dimensional space group. More information on these groups can be found in the supporting information and at https://gitlab.com/mcpe/tpmsgroups.

Funding information

MCP thanks the Villum Foundation for financial support through grant No. 22833.

References

Castelletto, V. & Hamley, I. W. (2004). *Curr. Opin. Solid State Mater. Sci.* **8**, 426–438.
Conway, J. H., Burgiel, H. & Goodman-Strauss, C. (2008). *The Symmetries of Things.* Wellesley, Massachusetts: CRC Press.
Delgado-Friedrichs, O. (2003). *Theor. Comput. Sci.* **303**, 431–445.
Delgado-Friedrichs, O. & O'Keeffe, M. (2003). *Acta Cryst.* A**59**, 351–360.
Dolan, J. A., Wilts, B. D., Vignolini, S., Baumberg, J. J., Steiner, U. & Wilkinson, T. D. (2015). *Adv. Opt. Mater.* **3**, 12–32.
Dress, A. W. (1987). *Adv. Math.* **63**, 196–212.
Epstein, D. B. A., Holt, D. F. & Rees, S. E. (1991). *J. Symbolic Comp.* **12**, 397–414.
Hyde, S. T. & Pedersen, M. C. (2021). *Proc. R. Soc. A.* **477**, 20200372.
Hyde, S. T., Ramsden, S. J. & Robins, V. (2014). *Acta Cryst.* A**70**, 319–337.
Kirkensgaard, J. J. K., Evans, M. E., de Campo, L. & Hyde, S. T. (2014). *Proc. Natl Acad. Sci. USA*, **111**, 1271–1276.
Mezzenga, R., Seddon, J. M., Drummond, C. J., Boyd, B. J., Schröder-Turk, G. E. & Sagalowicz, L. (2019). *Adv. Mater.* **31**, 1–19.
Pedersen, M. C. & Hyde, S. T. (2018). *Proc. Natl Acad. Sci. USA*, **115**, 6905–6910.
Pellé, A. & Teillaud, M. (2014). In 23rd International Meshing Roundtable (IMR23), Londres, UK. HAL Id: hal-01089967 https://hal.inria.fr/hal-01089967.
Robins, V., Ramsden, S. J. & Hyde, S. T. (2004). *Eur. Phys. J. B*, **39**, 365–375.
Sadoc, J.-F. & Charvolin, J. (1989). *Acta Cryst.* A**45**, 10–20.
Schoen, A. (1970). *Infinite Periodic Minimal Surfaces Without Self-intersections.* NASA.
Schwarz, H. A. (1890). Gesammelte mathematische Abhandlungen.
The GAP Group, (2021). *GAP – Groups, Algorithms, and Programming*. https://www.gap-system.org/.
Thurston, W. P. (1980). *The Geometry and Topology of Three-Manifolds.* Princeton: Princeton University.
Welch, P. M., Rasmussen, K. Ø. & Welch, C. F. (2019). *J. Chem. Phys.* **150**, 174905.